Available online at www.sciencedirect.com
ScienceDirect
Journal of Power Sources 162 (2006) 1282–1288
JOURNAL OF POWER SOURCES
www.elsevier.com/locate/jpowsour

Thermal reactions of mesocarbon microbead (MCMB) particles in $LiPF_6$-based electrolyte

Ang Xiao, Wentao Li, Brett L. Lucht *

University of Rhode Island, Department of Chemistry, Kingston RI 02881, USA

Received 23 June 2006; received in revised form 20 July 2006; accepted 21 July 2006
Available online 7 September 2006

Abstract

The thermal reaction of ternary electrolyte (1.0 M $LiPF_6$ in 1:1:1 ethylene carbonate/dimethyl carbonate/diethyl carbonate) with mesocarbon microbeads (MCMB) particles was investigated by the combined use of NMR, GC–MS, FTIR-ATR, TGA, XPS and SEM/EDS-element map. The thermal decomposition of ternary electrolyte is not inhibited by the presence of MCMB particles. The chemical composition and morphology of the surface of MCMB particles changes significantly upon storage in the presence of ternary electrolyte. Electrolyte decomposition products including oligocarbonates, oligoethylene oxides, polyethylene oxide (PEO), lithium fluorophosphates ($Li_xPO_yF_z$), and lithium fluoride are deposited on the surface of MCMB particles. The concentration of decomposition products on the surface of MCMB increases with increased storage time and temperature. The addition of dimethyl acetamide (DMAc) impedes the thermal decomposition of the electrolyte and deposition of electrolyte decomposition products on the surface of MCMB.

Keywords: Lithium-ion batteries; Electrolyte; Anode materials; Thermal stability; Capacity loss

1. Introduction

Lithium-ion batteries have rapidly become essential secondary batteries [1]. Lithium-ion batteries are widely used in cell phones, laptop computers, and other portable electronic devices and have recently become available for power tools. While the calendar life and thermal stability of lithium-ion batteries is adequate for these applications (5 years at an operational temperature of 0–40 °C), other applications, including hybrid electric vehicles (HEVs), electric vehicles (EVs), military, aerospace, and satellites, require significantly longer calendar life (10–15 years) and improved thermal stability (50–60 °C) [2,3]. Thus, identification of the mechanism of storage capacity loss and methods to prevent decreased performance are necessary to develop lithium-ion batteries with improved calendar life and elevated temperature performance. The loss of performance in lithium-ion batteries during accelerated aging experiments has been attributed to three factors; the continued reaction of the electrolyte with the anode (graphite or MCMB) or compounds present in the anode solid electrolyte interface (SEI) [4,5], decomposition of the electrolyte on the surface of cathode particles to generate resistive films [6–8], and bulk electrolyte decomposition [9–11].

The formation of SEI on anode particles in lithium-ion batteries is one of the most important factors in long-term cycling stability [12]. The SEI produced by reduction of electrolyte on the anode is beneficial to the performance of lithium-ion batteries. However, the long-term thermal stability of the SEI is questionable. Recent investigations suggest that the anode SEI layer undergoes an alternating deterioration and reformation process at elevated temperature in the presence of $LiPF_6$-based electrolyte [4]. It has been proposed that the surface film reacts with electrolyte at elevated temperature to form thicker, more resistive films with high concentrations of $LiPF_6$ decomposition products [13,14]. However, the structure of the anode SEI is not fully understood. In addition, the presence of binder, typically PVDF, and other additives make a quantitative understanding of the compositional changes occurring on the surface of the anode as a function of time and temperature difficult.

Therefore, as part of our investigation of the thermal decomposition reactions of lithium-ion battery components [15–18], we have conducted a detailed investigation of the

* Corresponding author. Tel.: +1 401 874 5071; fax: +1 401 874 5072.
E-mail address: blucht@chm.uri.edu (B.L. Lucht).

0378-7753/$ – see front matter © 2006 Elsevier B.V. All rights reserved.
doi:10.1016/j.jpowsour.2006.07.054

thermal reactions of MCMB particles with $LiPF_6$ in 1:1:1 EC/DEC/DMC. Developing a basic understanding of the thermal reactions that occur between graphite (MCMB) and electrolyte ($LiPF_6$ in EC/DMC/DEC) will provide a foundation for further investigation of the reaction between the SEI and electrolyte. In this report, nuclear magnetic resonance spectroscopy (NMR), gas chromatography with mass selective detection (GC–MS), fourier transform infrared spectroscopy in the attenuated total reflection mode (FTIR-ATR), thermogravimetric analysis (TGA), X-ray photoelectron spectroscopy (XPS) and scanning electron microscopy with energy dispersive X-ray spectroscopy and element map (SEM/EDS-element map) were used to monitor both electrolyte and MCMB particles after storage.

2. Experimental

Glass vials were charged with 0.3 g of MCMB particles and 0.9 g of 1.0 M $LiPF_6$ in 1:1:1 EC/DEC/DMC (ternary electrolyte, from EM Industries without further purification) with and without 3 wt.% dimethyl acetamide (DMAc). All samples were prepared inside a nitrogen-filled glove box and flame sealed on a vacuum line. The sealed vials were then stored at room temperature or at 85 °C in an oil bath for 4, 7 and 10 days. After storage the vials were opened inside the nitrogen-filled glove box. Both the solid and liquid portions were analyzed. All solid samples were washed three times with DMC to remove $LiPF_6$ and then evacuated overnight at room temperature to remove residual DMC.

The liquid electrolyte was analyzed by nuclear magnetic resonance spectroscopy. NMR spectra were acquired on a JEOL 400 MHz NMR spectrometer. ^1H NMR resonances were referenced to EC at 4.51 ppm. ^{19}F NMR resonances were referenced to $LiPF_6$ at 65.0 ppm. The initial concentration of HF and fluorophosphates (OPF_2OR) resulting from trace protic impurities, such as water, was below the detectable limit (50 ppm) by ^{19}F NMR spectroscopy for all electrolytes investigated [17,19]. The wash DMC was analyzed by gas chromatography with mass selective detection. analyses were obtained on an Agilent Technologies 6890GC with a 5973 Mass Selective Detector and a HP-5MS Column. Helium was used as the carrier gas with a flow rate of 3.3 mL/min. Samples were ramped from 50 to 250 °C at 10 °C/min.

All solid samples were analyzed by fourier transform infrared spectroscopy (FTIR), thermalgravimetric analysis, X-ray photoelectron spectroscopy (XPS), scanning electron microscopy (SEM) and energy dispersive X-ray spectroscopy (EDS) with elemental map. The FTIR measurements were obtained on a Thermo Nicolet IR 300 spectrometer inside the nitrogen-purged glove bag. The spectra were acquired in the attenuated total reflection (ATR) mode with the resolution 4 cm^{-1} and total 128 scans. Thermal behaviors of the solid were analyzed on TA instruments SDT 2900. The temperature was ramped from room temperature to 600 °C. The XPS spectra were obtained by a PHI 5500 system using Al Kα radiation ($h\nu = 1486.6$ eV) under ultra high vacuum. Lithium was not monitored due to its low inherent sensitivity and small change of binding energy. SEM and EDS with elemental map analyses were conducted on a JEOL-5900 scanning electron microscope.

3. Results and discussion

3.1. Analysis of electrolyte solution

3.1.1. ^1H and ^{19}F NMR

Ternary electrolyte with and without added DMAc was stored in the presence of MCMB particles at room temperature and 85 °C. After storage the electrolyte was analyzed by ^1H and ^{19}F NMR spectroscopy. Samples stored at room temperature contained ^1H and ^{19}F resonances characteristic of the electrolyte but did not contain resonances characteristic of decomposition products. Samples without DMAc stored at 85 °C for 4 days contained ^1H and ^{19}F resonance characteristic of decomposition products. Ester exchange reactions between DMC and DEC produce EMC as observed by ^1H NMR spectroscopy (q, 4.13 ppm and s, 3.71 ppm) while ^{19}F NMR spectra contained resonances consistent with fluorophosphoric acid (OPF_2OH, d, 54.4 ppm), diethylfluorophosphate (OPF_2OEt, d, 53.1 ppm) and dimethylfluorophosphate (OPF_2OMe, d, 51.2 ppm). OPF_2OEt and OPF_2OMe are the intermediate products of autocatalytic reaction of electrolyte decomposition. OPF_2OH can be generated from the elimination reaction of OPF_2OEt. Continued storage of ternary electrolyte at 85 °C for 10 days leads to further decomposition of the electrolyte. New resonances characteristic of OPF_3, $OPF(OH)_2$, OPF(OMe)(OEt), OPF(OMe)(OH), OPF(OEt)(OH), $OPF(OEt)_2$, and $OPF(OMe)_2$ are observed as previously characterized [11,17]. Samples of ternary electrolyte with 3 wt.% added DMAc contain no evidence of decomposition products by ^1H or ^{19}F NMR spectroscopy after storage for 10 days at 85 °C. DMAc significantly decreases the rate of thermal decomposition of the electrolyte in the presence of MCMB.

The effect of DMAc on the thermal decomposition of ternary electrolyte in the absence of MCMB was also investigated. Ternary electrolyte sealed in glass NMR tubes and stored at 85 °C for 5 days results in the conversion of approximately 10% of the $LiPF_6$ to OPF_2OR and other decomposition products [17]. Continued storage at 85 °C for 4 weeks results in nearly quantitative decomposition of $LiPF_6$. Addition of 3 wt.% DMAc to ternary electrolyte completely inhibits the thermal decomposition. While storage of ternary electrolyte with 3 wt.% DMAc at 85 °C results in the formation of low concentrations of POF_2OLi (less than 0.5%) during the first few days of storage, the concentration does not increase upon storage at 85 °C for up to 18 months. Previous investigations of related Lewis basic additives, including pyridine and hexamethylphosphoramide (HMPA), have confirmed the mechanism of inhibition of the thermal decomposition of $LiPF_6$/carbonate based electrolytes [15]. The presence of base-PF_5 complexes inhibits the thermal decomposition of $LiPF_6$ by reversibly sequestering free PF_5 and preventing the subsequent reaction with organic carbonates.

$$LiPF_6 \overset{\Delta}{\rightleftharpoons} LiF + PF_5 \overset{DMAc}{\rightleftharpoons} DMAc\text{–}PF_5 \quad (1)$$

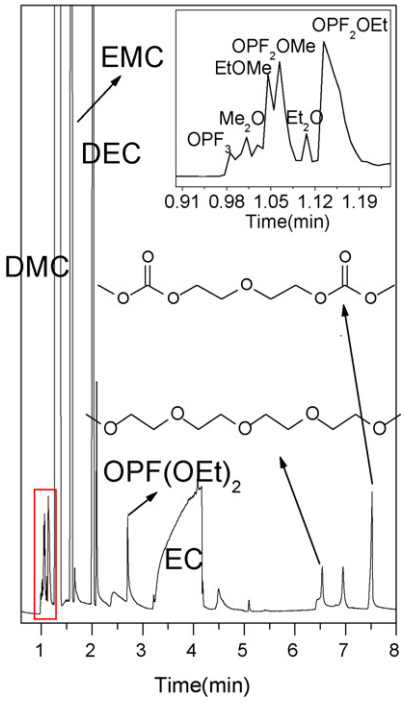

Fig. 1. Gas chromatogram of washing liquid for sample stored for 10 days at 85 °C.

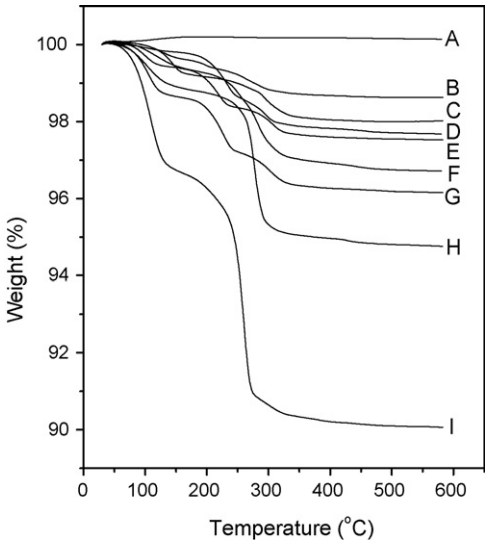

Fig. 2. Thermogravimetric analysis plots for all samples: (A) fresh MCMB; (B) 10 days at RT with DMAc; (C) 10 days at 85 °C with DMAc; (D) 4 days at RT; (E) 7 days at RT; (F) 4 days at 85 °C; (G) 10 days at RT; (H) 7 days at 85 °C and (I) 10 days at 85 °C.

3.1.2. GC–MS

After storage and separation of the liquid electrolyte from the solid MCMB particles, the MCMB particles were rinsed with DMC to dissolve soluble decomposition products adhering to the surface. The volatile components of the DMC extract were analyzed by GC–MS and structurally assigned through matching to the National Institutes of Standards (NIST) library. Extracts from samples stored at room temperature contained no decomposition products. However, extracts from samples containing ternary electrolyte without added DMAc stored at elevated temperature contained many new species. Decomposition products observed in samples stored for 10 days at 85 °C include CO_2, Me_2O, EtOMe, OPF_2OMe, Et_2O, OPF_2OEt, $OPF(OEt)_2$ (Fig. 1), as previously reported for the thermal decomposition of pure electrolytes [17]. In addition, we observed significant concentrations of oligocarbonates and oligoethylene oxides, products that were observed at very low concentration in the thermal decomposition of pure ternary electrolyte, suggesting that the oligomerization reactions may be mediated by the surface of the MCMB. Extracts from samples containing ternary electrolyte with 3% DMAc stored for 10 days at 85 °C contain no decomposition products.

3.2. Analysis of MCMB particles

3.2.1. TGA

Thermal gravimetric analysis was used to investigate the presence of volatile organic compounds on the surface of MCMB [20–22]. The thermal behaviors of MCMB stored in the presence of ternary electrolyte under various conditions are shown in Fig. 2 and the total weight losses are summarized in Table 1.

There are three clear trends in weight loss. First, an increase in the storage temperature results in an increase in the weight loss. This is observed when comparing curves D (4 days at RT) and F (4 days at 85 °C) or G (10 days at RT) and I (10 days at 85 °C). Thus, more electrolyte decomposition products are deposited on the surface of the MCMB at higher temperatures. Second, increased storage time results in more weight loss, and consequently more electrolyte deposition products, as evidenced with curves D, E, and G (samples stored at RT for 4, 7, and 10 days, respectively). Finally, samples with added DMAc (curve B and C) have the least weight loss. The sample with 3% DMAc stored at 85 °C for 10 days (curve C) loses less weight than particles stored without DMAc for 7 days at either room temperature (curve E) or at 85 °C (curve H). Some of the observed weight loss may be due to residual DMC or EC retained in the pores of the MCMB, but the observed trends in weight loss are consistent with increases in the deposition of electrolyte decomposition products as a function of storage time and temperature. The addition of 3% DMAc should not change the adsorption/retention of carbonate solvents in the MCMB.

Table 1
Weight loss of all samples by TGA

Samples	Weight loss (%)
Fresh MCMB	0
MCMB, 10 d at RT with DMAc	1.4
MCMB, 10 d at 85 °C with DMAc	2.0
MCMB, 4 d at RT	2.3
MCMB, 7 d at RT	3.5
MCMB, 4 d at 85 °C	3.3
MCMB, 10 d at RT	3.8
MCMB, 7 d at 85 °C	5.2
MCMB, 10 d at 85 °C	9.9

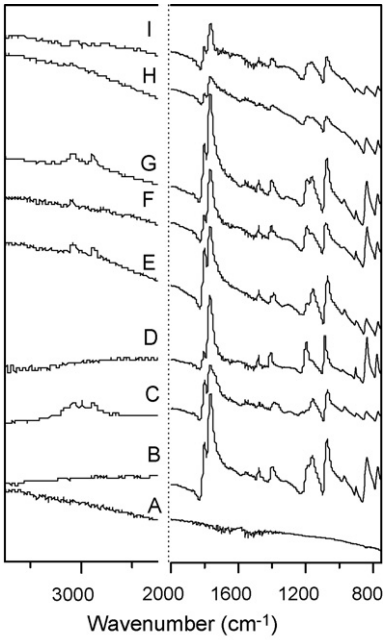

Fig. 3. IR spectra of all samples: (A) fresh MCMB; (B) 4 days at RT; (C) 4 days at 85 °C; (D) 7 days at RT; (E) 7 days at 85 °C; (F) 10 days at RT; (G) 10 days at 85 °C; (H) 10 days at RT with DMAc and (I) 10 days at 85 °C with DMAc.

3.2.2. FTIR-ATR

The IR spectra of MCMB particles stored in the presence of electrolyte are shown in Fig. 3. The two IR frequency regions of most interest for electrolyte decomposition products are C–H stretching at 3000–2700 cm^{-1} and 1800–1600 cm^{-1} for the C=O stretching vibration [23–26]. While some of the absorptions are consistent with small quantities of residual EC in the MCMB, the spectral changes as a function of storage time, temperature and addition of DMAc are discussed below. Spectra of samples stored at high temperature have significant absorptions between 2800 and 3200 cm^{-1}, while samples stored at room temperature contain weak absorptions in this region. The increase in intensity is consistent with more C–H containing species, most likely oligocarbonate and oligoethylene oxides from decomposition of electrolyte, after high temperature storage. The strong carbonyl absorptions centered at 1767 and 1800 cm^{-1} are attributed to C=O stretching from carbonates. With the increase of temperature, the intensity of peak at 1800 cm^{-1} increases from a small shoulder to an independent peak which coincides with an increase in the intensity of absorption between 3000 and 2700 cm^{-1}. The changes of IR spectra support increasing deposition of electrolyte decomposition products with temperature. Incorporation of DMAc significantly impedes the deposition of electrolyte decomposition products. After storage for 10 days at 85 °C, the carbonyl absorptions at 1767 and 1800 cm^{-1} have low intensity and the absorptions between 3000 and 2700 cm^{-1} are negligible.

3.2.3. XPS

The influence of storage time and temperature on the surface of MCMB was further investigated by X-ray photoelectron spectroscopy. A systematic change in the XPS spectra (C 1s, O 1s, and F 1s) is observed for samples stored at 85 °C for 4, 7 and 10 days (Figs. 4A–C and 5). Surface atomic concentrations (C, F, P, and O) for samples stored at 85 °C are shown in Fig. 5. The relative atomic concentration of C decreases while O, F and P increase with additional storage time. A similar trend is observed for samples stored at room temperature. This indicates that electrolyte decomposition products, species containing O, F and P, are being deposited on the surface of MCMB as a function of storage time. Further examination of individual spectra for each element provides additional insight into film growth. Examination of the C 1s spectra reveals two primary components at 284 and 286.5 eV, consistent with carbon in alkanes/graphite (C–C) and ethers (C–O) [27–29]. The peak characteristic of

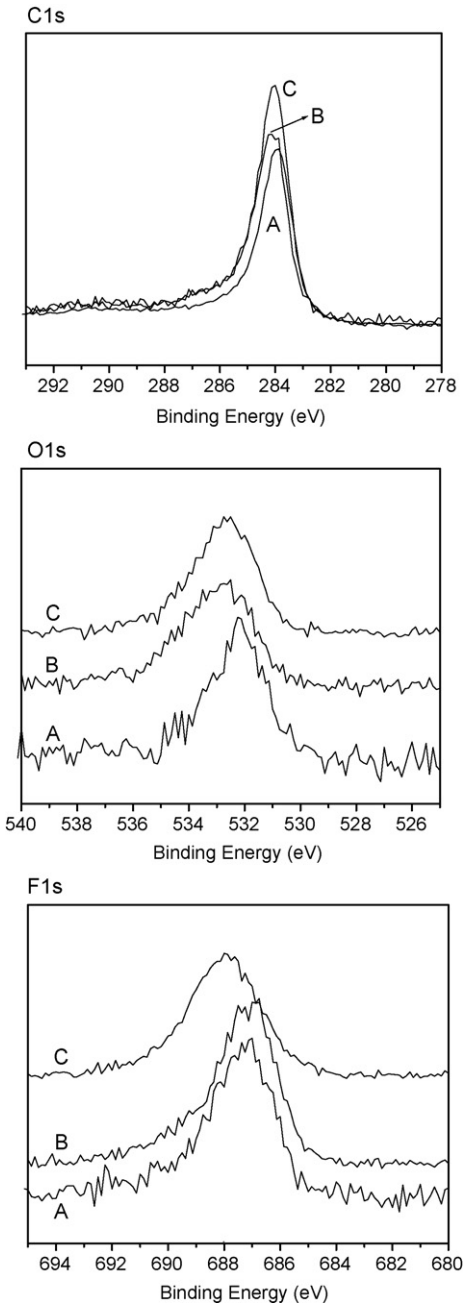

Fig. 4. XPS spectra of samples at 85 °C: (A) 4 days; (B) 7 days and (C) 10 days.

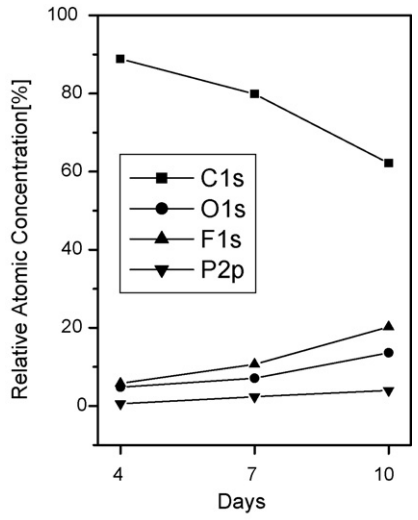

Fig. 5. Relative atomic concentration of samples at 85 °C.

C–O linkages increases with increased storage time at 85 °C. Detailed analysis of the O 1s spectra also reveals two primary components at 531 and 533 eV corresponding to oxygen in carbonates and ether linkages. As storage time is increased from 4 to 10 days, the O 1s peak shifts from 531 to 533 eV, suggesting a gradual shift from carbonates to ethers. The presence of C–O linkages, as evidenced in C 1s and O 1s spectra, is most likely due to oligo and polyethylene oxides which increase as a function of storage time due to decarboxylation of the related carbonates [30]. Similar results were observed by GC–MS as discussed above. Analysis of the F 1s chemical state reveals two peaks at 687, and 688 eV. The peak at 687 is assigned to residual $LiPF_6$ on the surface of MCMB while peak at 688 is assigned to lithium fluorophosphates $Li_xPO_yF_z$. The intensity shifts from 687 to 688 eV upon increase storage time supporting the formation of fluorophosphate decomposition products ($Li_xPO_yF_z$) as a function of storage time.

Samples of MCMB stored in ternary electrolyte with 3 wt.% of DMAc were analyzed by XPS. Compared to samples without added DMAC, the atomic concentration of C is higher and the atomic concentrations of O, F, and P are lower. A comparison of XPS spectra of C 1s, O 1s, and F 1s, respectively for samples with and without DMAc stored for 10 days at 85 °C is shown in Fig. 6. While the changes in the C 1s and O 1s spectra are subtle, the C 1s peak at 286 and O 1s peak at 533, both characteristic of C–O linkages, have lower intensity. In addition, samples containing DMAc have negligible intensity at 688 eV suggesting little $Li_xPO_yF_z$ on the surface of MCMB. Most of the surface fluorine is LiF (F 1s, 686 eV). The addition of DMAc clearly inhibits the deposition of electrolyte decomposition products, oligo or polyethylene oxide and lithium fluorophosphates, on the surface of MCMB.

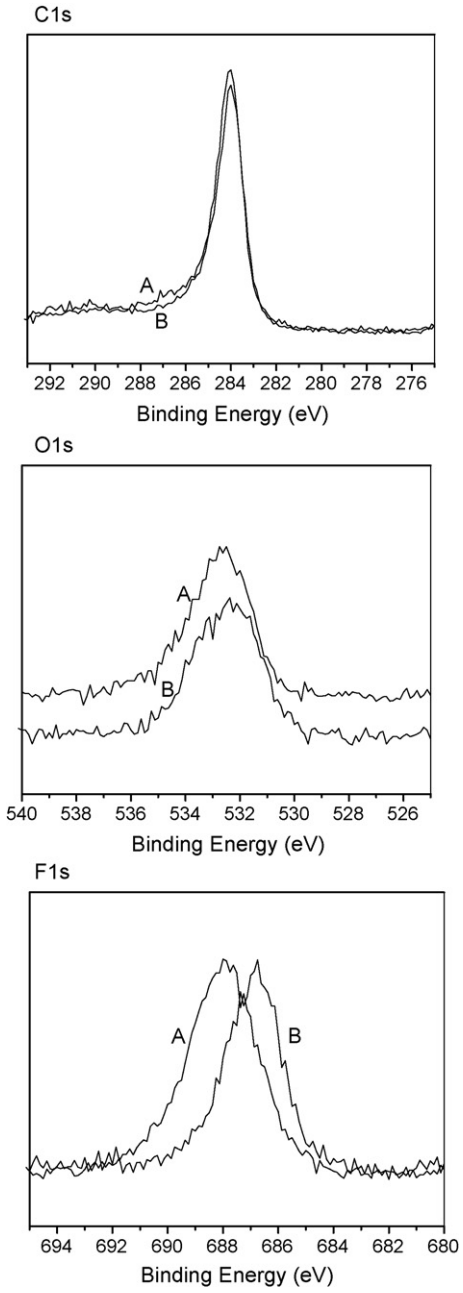

Fig. 6. XPS spectra of samples stored for 10 days at 85 °C: (A) additive free and (B) with additive.

3.2.4. SEM/EDS-site map

The surface of MCMB particles stored in the presence of ternary electrolyte was further investigated with scanning electron microscopy. Fig. 7a and b shows micrographs of samples stored for 4 days at room temperature and 10 days at 85 °C. The surface on the individual graphite particles is rough with primary particles ranging in size from 1 to 10 μm. In addition to the MCMB particles, there are some regions of amorphous materials, observed as white regions in the SEM images. The concentration of the amorphous regions is significantly greater in samples that have been stored at 85 °C. EDS indicates that the white amorphous regions contain carbon, oxygen, fluorine, and phosphorus which result from the decomposition of electrolyte.

The secondary X-ray image and elemental site maps for MCMB stored with ternary electrolyte at room temperature for 4 days and 85 °C for 10 days are provided in Fig. 8a and b. While

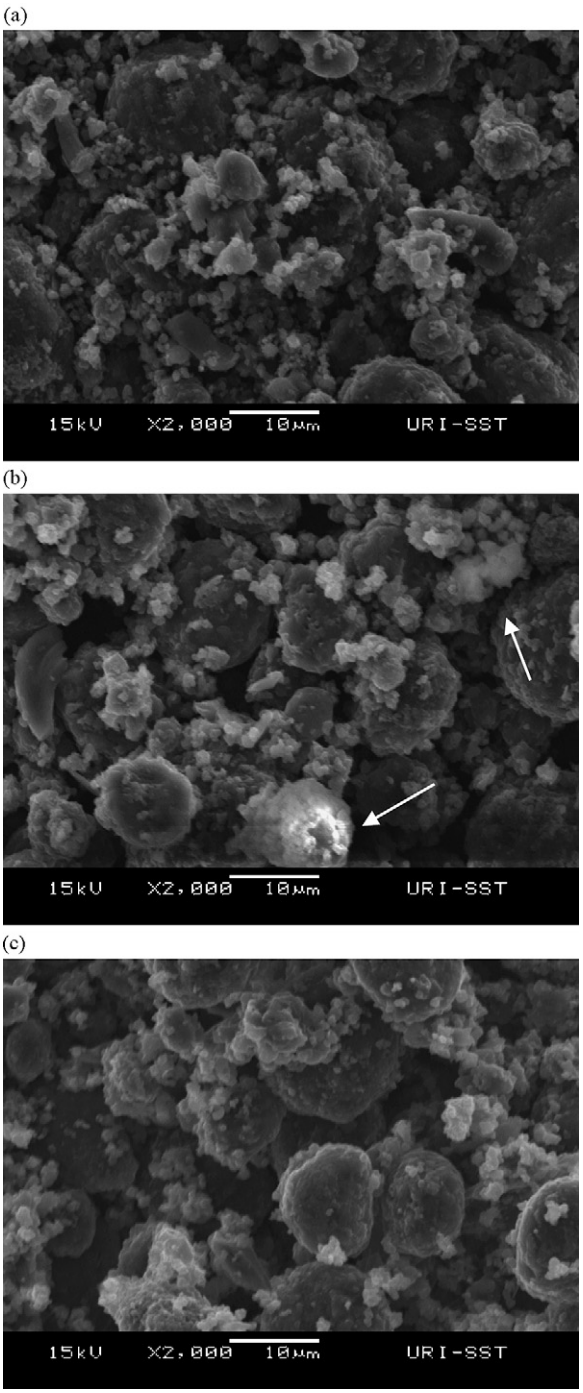

Fig. 7. SEM micrographs of MCMB particles surface: (a) 4 days at RT; (b) 10 days at 85 °C; (c) 10 days at 85 °C with 3% DMAc.

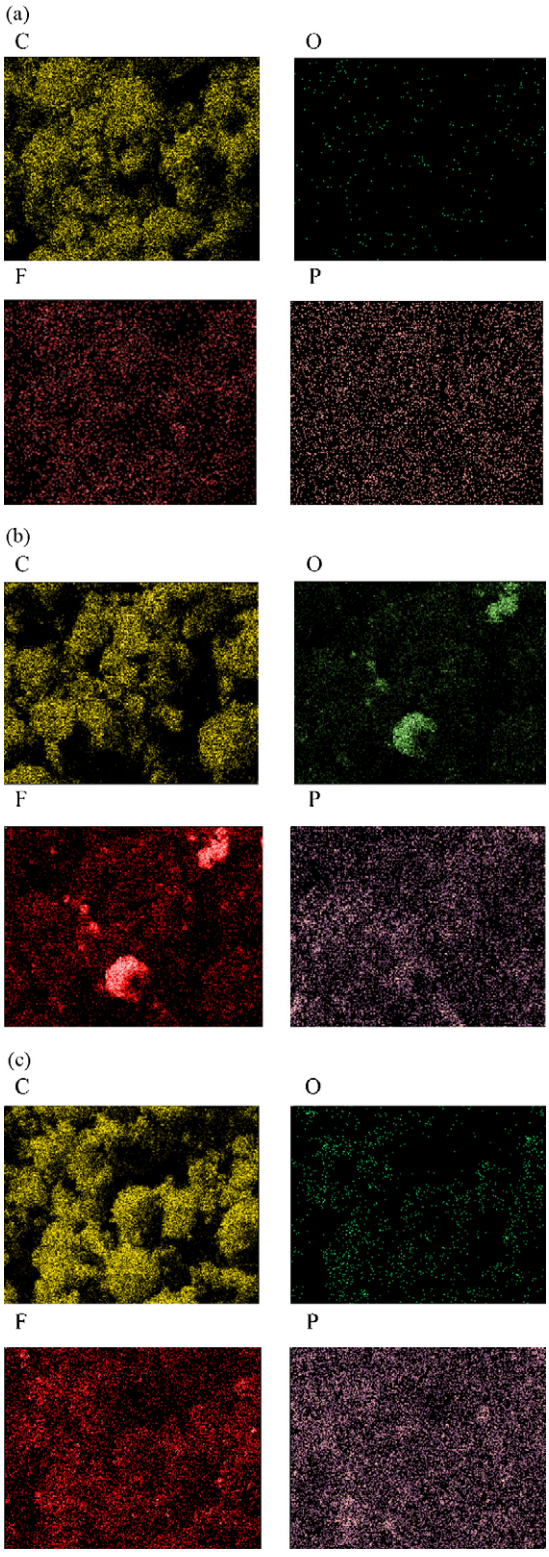

Fig. 8. Element maps of MCMB stored in the presence of ternary electrolyte: (a) 4 days at RT; (b) 10 days at 85 °C; (c) 10 days at 85 °C with 3% DMAc.

the X-ray image has poorer resolution than the than secondary electron image, the element maps show the spatial distribution of C, O, F, and P. The brighter regions in the element map indicate greater X-ray intensity and higher elemental concentration. The sample stored at room temperature for 4 days is primarily composed of carbon. Low concentrations of oxygen, fluorine, and phosphorus uniformly cover the graphite particles. Samples stored at room temperature have little deposition of electrolyte degradation products. However, after storage at 85 °C for 10 days the surface of the MCMB particles is significantly modified. In addition to the spherical-like graphite particles composed of C, there are large areas that contain high concentrations of O, F, and P, consistent with electrolyte decomposition products. The presence of high concentrations of electrolyte decomposition

products in "pockets" on the surface could result from defect sites on MCMB catalyzing electrolyte decomposition or non-uniform dissolution of the decomposition products during the DMC wash.

Samples of MCMB stored in the presence of ternary electrolyte with 3% DMAc were also analyzed by SEM and EDS (Figs. 7c and 8c). The SEM images of samples stored at 85 °C with added DMAc contain less amorphous white regions on the surface of the MCMB than samples without DMAc. The element maps for samples containing DMAc have much less O, F, and P than comparable samples without DMAc. The SEM and EDS results further confirm the inhibition of electrolyte decomposition on the surface of MCMB by DMAc.

4. Conclusion

A detailed analysis of the thermal reactions between MCMB and ternary electrolyte (1.0 M $LiPF_6$ in EC/DEC/DMC) has been conducted with GC–MS, NMR, TGA, XPS, and SEM with EDS. All of the techniques provide corroborating results. Storage of MCMB in the presence of ternary electrolyte at elevated temperature results in thermal decomposition of the electrolyte and deposition of electrolyte decomposition products on the surface of the MCMB. The rate of electrolyte decomposition and product distribution are similar to those previously reported for the thermal decomposition of pure ternary electrolyte. The primary components on the surface of the MCMB include oligocarbonates, oligoethylene oxide, polyethylene oxide (PEO), fluorophosphates, and lithium fluoride. The appearance of the organic components, oligocarbonates, oligoethylene oxides, and PEO most likely results form ring opening reactions of ethylene carbonate. These ring opening reactions can be mediated by Lewis acidic species, such as PF_5 [30], or reactive surface sites on the MCMB. The presence of lithium fluorophosphates ($Li_xPO_yF_z$) results from the thermal decomposition of $LiPF_6$. The concentration of both the organic and inorganic components of the surface films increase as a function of time and temperature. Higher temperatures and longer storage times lead to more decomposition products and the thicker surface films.

The addition of the thermal stabilizing additive DMAc impedes the thermal decomposition of the electrolyte and the deposition of electrolyte decomposition products on the surface of MCMB. DMAc impedes the thermal decomposition by reversibly sequestering the Lewis acidic PF_5, generated via the thermal dissociation of $LiPF_6$, and circumventing the autocatalytic decomposition of the electrolyte. Inhibition of the electrolyte decomposition reduces the deposition of surface species on MCMB. Investigation of the effect of DMAc on the thermal stability of lithium-ion cells is in progress and will be reported in due course.

Acknowledgements

We thank the NSF/CIA (Award no. DMR-0442024) for financial support of this research. We thank Michael Platek and the Sensors and Surface Technology Partnership at the University of Rhode Island for assistance with the XPS and SEM.

References

[1] W.A. Van Schalkwijk, B. Scrosati (Eds.), Advances in Lithium-Ion Batteries, Kluwer Academic Press, New York, 2002.
[2] G. Sarre, P. Blanchard, M. Broussely, J. Power Sources 127 (2004) 65.
[3] D.P. Abraham, J. Liu, C.H. Chen, Y.E. Hyung, M. Stoll, N. Elsen, S. Maclaren, R. Twesten, R. Haasch, E. Sammann, I. Petrov, K. Amine, G. Henriksen, J. Power Sources 119–121 (2003) 511.
[4] H.H. Lee, C.C. Wan, Y.Y. Wang, J. Electrochem. Soc. 151 (2004) A542.
[5] M. Herstedt, D.P. Abraham, J.B. Kerr, K. Edstrom, Eletrochem. Acta 49 (2004) 5097.
[6] D.P. Abraham, R.D. Twesten, M. Balasubramanian, J. Kropf, D. Fishcher, J. McBreen, I. Petrov, K. Amine, J. Electrochem. Soc. 150 (2003) A1450.
[7] A.M. Andersson, D.P. Abraham, R. Haasch, S. MacLaren, J. Liu, K. Amine, J. Electrochem. Soc. 149 (2002) A1358.
[8] D. Aurbach, K. Gamolsky, B. Markovsky, G. Salitra, Y. Gofer, U. Heider, R. Oesten, M. Schmidt, J. Electrochem. Soc. 147 (2000) 1322.
[9] K. Xu, Chem. Rev. 104 (2004) 4303.
[10] S.E. Sloop, J.B. Kerr, K. Kinoshita, J. Power Sources 119–121 (2003) 330.
[11] B. Ravdel, K.M. Abraham, R. Gitzendanner, J. Dicarlo, B.L. Lucht, C. Campion, J. Power Sources 119–121 (2003) 805.
[12] D. Aurbach, B. Markovsky, A. Shechter, Y. Ein-Eli, H. Cohen, J. Electrochem. Soc. 143 (1996) 3809.
[13] P. Aora, R.E. White, M. Doyle, J. Electrochem. Soc. 145 (1998) 3647.
[14] Y. Wang, X. Guo, S. Greenbaum, J. Liu, K. Amine, Electrochem. Solid-State Lett. 4 (2001) A68.
[15] W. Li, C. Campion, B.L. Lucht, B. Ravdel, J. DiCarlo, K.M. Abraham, J. Electrochem. Soc. 152 (2005) A1361.
[16] C. Campion, W. Li, W.E. Euler, B.L. Lucht, B. Ravdel, J. DiCarlo, R. Gitzendanner, K.M. Abraham, Electrochem. Solid-State Lett. 7 (2004) A194.
[17] C. Campion, W. Li, B.L. Lucht, J. Electrochem. Soc. 152 (2005) A2327.
[18] W. Li, B.L. Lucht, J. Electrochem Soc. 153 (2006) A1617.
[19] T. Kawamura, S. Okada, J.-I. Yamaki, J. Power Sources 156 (2006) 547.
[20] A.Du. Pasquier, F. Disma, T. Bowmer, A.S. Gozdz, G. Amatucci, J.-M. Tarascon, J. Electrochem. Soc. 145 (1998) 472.
[21] E.P. Roth, D.H. Doughty, J. Power Sources 128 (2004) 308.
[22] E.P. Roth, D.H. Doughty, J. Franklin, J. Power Sources 134 (2004) 222.
[23] S.-W. Song, G.V. Zhuang, P.N. Ross, J. Electrochem. Soc. 151 (2004) A1162.
[24] G.V. Zhuang, P.N. Ross, Electrochem. Solid-State Lett. 6 (2003) A136.
[25] G.V. Zhuang, H. Yang, B. Blizanac, P.N. Ross, Electrochem. Solid-State Lett. 8 (2005) A441.
[26] G. Chen, G.V. Zhuang, T.J. Richardson, G. Liu, P.N. Ross, Electrochem. Solid-State Lett. 8 (2005) A344.
[27] A.M. Andersson, K. Edstrom, J. Electrochem. Soc. 148 (2001) A1100.
[28] T. Eriksson, A.M. Andersson, A.G. Bishop, C. Gejke, T. Gustafsson, J.O. Thomas, J. Electrochem. Soc. 149 (2002) A69.
[29] A.M. Andersson, M. Herstedt, A.G. Bishop, K. Edstrom, Eletrochem. Acta 47 (2002) 1885.
[30] L. Vogdanis, B. Martens, H. Uchtmann, F. Hensel, W. Heitz, Makromol. Chem. 191 (1990) 465.